Electronic Supplementary Material (ESI) for ChemComm.

Electronic Supplementary Material

Highly active oxygen reduction reaction on Fe-nanoclustered hierarchical porous carbon derived from CO_2

Ayeong Byeon, Hodong Kim, Jae Hyun Park, Gi Mihn Kim, and Jae W. Lee*

Department of Chemical and Biomolecular Engineering, Korea Advanced Institute of Science and Technology (KAIST), Daejeon 305-701, Republic of Korea

*Corresponding author. Tel: +82-42-350-3940. E-mail: jaewlee@kaist.ac.kr

Experimental

Argon (Ar, > 99.9%) and carbon dioxide (CO_2, > 99.9%) were purchased from Deokyang Co., Ltd. Sodium borohydride ($NaBH_4$, > 99%), polytetrafluoroethylene (PTFE, 60 wt% dispersion in water), and potassium hydroxide (KOH, > 90%), Iron chloride tetrahydrate ($FeCl_2 \cdot 4H_2O$, >99.0%), Pt/C 20 wt.% (Platinum on graphitized carbon), Nafion® perfluorinated resin solution (5 wt.% in lower aliphatic alcohols and water; contains 15–20 % water) were purchased from Sigma-Aldrich. Hydrochloric acid (HCl, 37 wt% in water) was available in Junsei Chemical Co., Ltd. Ammonia solution (NH_4OH, 25-30 %) was purchased from Samchun. Calcium carbonate nanoparticles ($CaCO_3$, 15 - 40 nm) were acquired from SkySpring Nanomaterials. All of the chemicals were used without further purification.

4 g of $NaBH_4$ was mechanically mixed with $CaCO_3$ with relative weight of 1:2 for CPC. The mixed powder was heat treated under CO_2 at 500 ℃ (5 ℃/min) and maintained at this temperature for 2 hr, and then the gas was switched to Ar at 600 ℃ and heated up to 700 ℃ (5 ℃/min) and maintained at this temperature for another 2 hr. The resulting black solid residue was treated with 5 M HCl to remove unwanted salt with heating at 80 ℃ for 2 hr and then was rinsed with DIW thoroughly several times and dried at 80 ℃ overnight. Around 0.24 g of CPC was obtained after drying with a yield of ca. 5 -6 % based on the initial amounts of $NaBH_4$.

The CPC powder was heated under bubbling of ammonia solution with Ar as a carrier gas at 850 ℃ (5 ℃/min) for 1 hr for CPC-NH3. The CPC powder was impregnated with $FeCl_2 \cdot 4H_2O$ in DIW with the relative amounts of 1.98 wt.% and 200 wt.% for CPC-Fe-NC and CPC-Fe-NP, respectively. After sonication for 30 min, the slurry was dried at 80 ℃ overnight. The dried powder was heat treated under ammonia at 850 ℃ (5 ℃/min) for 1 hr for CPC-Fe-NC and CPC-Fe-NP.

Characterization

Powder X-ray diffraction data was obtained by a SmartLab (Rigaku, Japan) with Cu Kα radiation at 9 kW at a scan rate of 5° min^{-1}. Scanning electron microscope (SEM) was used to investigate the morphology using SU5000 (Hitachi, Japan). Field emission transmission electron microscope (TEM) was used to observe micro morphology and lattice fringes with Tecnai F20 (FEI Company, America). The X-ray photoelectron spectroscopy (XPS) data was provided by K-alpha (Thermo VG Scientific, America) with Al (1386.7 eV) as a X-ray source. Brunauer-Emmeett-Teller (BET) surface area was determined by N_2 adsorption-desorption isotherms at 77 K from TriStar II 3020 (Micrometritics). The pore size distribution was derived from the BJH theory. The micropore volume (V_{micro}) was determined with the t-plot method. Elemental analysis (EA) was performed by a Thermo Fisher Scientific FlashSmart.

Electrochemical Measurement

The catalyst ink was consisted of 4 mg of catalyst powder, 100 ul of Nafion® solution, and 1 ml of ethanol. After vigorous sonication, 8 ul of solution was deposited onto the surface of RDE electrode (dia. = 3 mm) and 12 ul for RRDE electrode (dia. = 4 mm). The electrode was tested with three electrode system consisting of working electrode, Ag/AgCl as a reference electrode and platinum wire as counter electrode. The cyclic voltammogram (CV) was obtained with the scan rate of 50 mV/s with the potential range of 1 V. The linear sweep voltammetry (LSV) was measured with rotating rate of 500, 1000, 1500, 2000, and 2500 rpm. From RRDE measurement, hydrogen peroxide yield (%) and electron transfer number (n) are

obtained through the equation below:

$$H_2O_2\,(\%) = \frac{200 \times I_{ring}}{N \times I_{disk} + I_{ring}}$$

$$n = \frac{4 \times I_{disk}}{I_{disk} + I_{ring}/N}$$

where, I_{disk} is absolute value of disk current, I_{ring} is ring current, N is current collection efficiency which is 0.424 in this work,

To obtain Tafel slope, Koutechy-Levich (K-L) equation was obtained:

$$\frac{1}{J} = \frac{1}{J_L} + \frac{1}{J_K} = \frac{1}{B\omega^{1/2}} + \frac{1}{J_K}$$

$$B = 0.62nFC_0D^{2/3}\upsilon^{-1/6}$$

$$\eta = a + b\,log\,J_k$$

Where, J is current density, J_L is diffusion-limiting current density, J_k is kinetic-limiting current density, F is Faraday constant (96500 C/mol). C_0 is the bulk concentration of 0.1 M KOH ($1.26*10^{-6}$ mol/cm^3), D is the diffusion coefficient of O_2 ($1.93*10^{-5}$ cm^2/s), ν is the kinematic viscosity of the electrolyte ($1.09*10^{-2}$ cm^2/s), I_k is kinetic current density, b is Tafel slope, ω is rotation rate (rpm).

The electrochemical cycle stability for CPC-Fe-NC and Pt/C 20 wt.% was measured with Linear sweep voltammetry after cycling 8000 times with potential range of 0 to -0.6 V vs. Ag/AgCl.

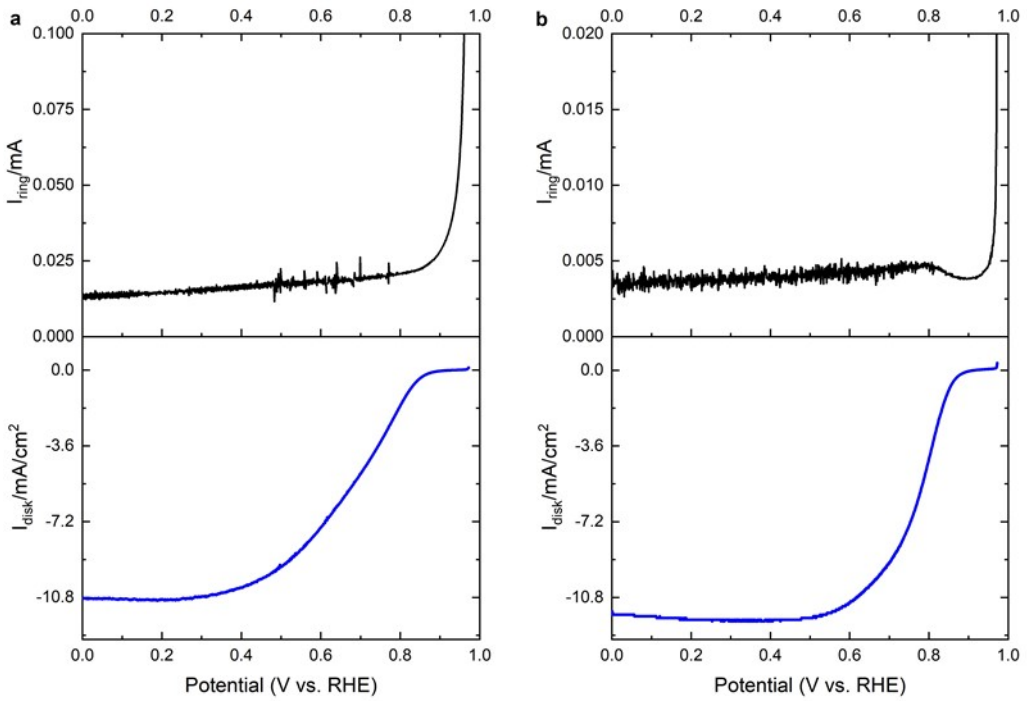

Figure S1. (a,b) RRDE curves of CPC-Fe-NC and Pt/C 20 wt% under in 0.1 M KOH at rotating rate of 1600 rpm in 0.1 M KOH.

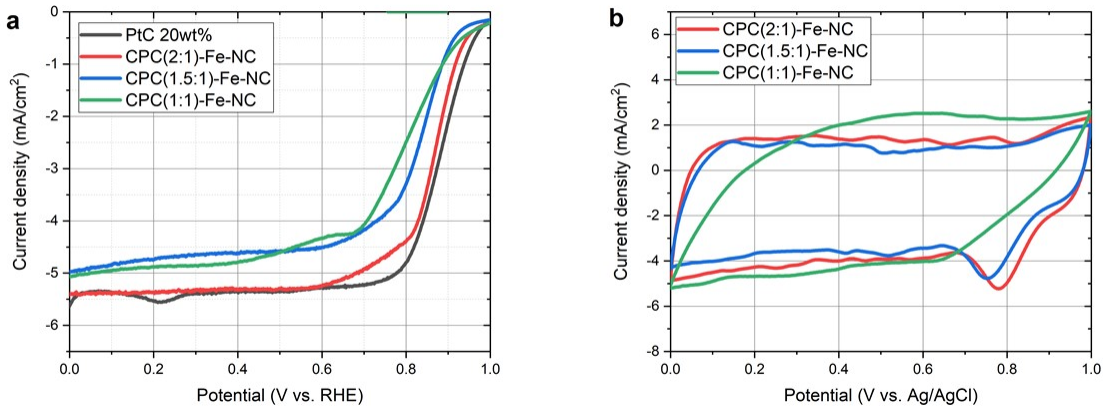

Figure S2. (a) LSV curves of Pt/C 20 wt.%, CPC(2:1)-Fe-NC, CPC(1.5:1)-Fe-NC, and CPC(1:1)-Fe-NC at 1500 rpm in 0.1 M KOH, and (b) CV curves of Pt/C 20 wt.%, CPC(2:1)-Fe-NC, CPC(1.5:1)-Fe-NC, and CPC(1:1)-Fe-NC in 0.1 M KOH.

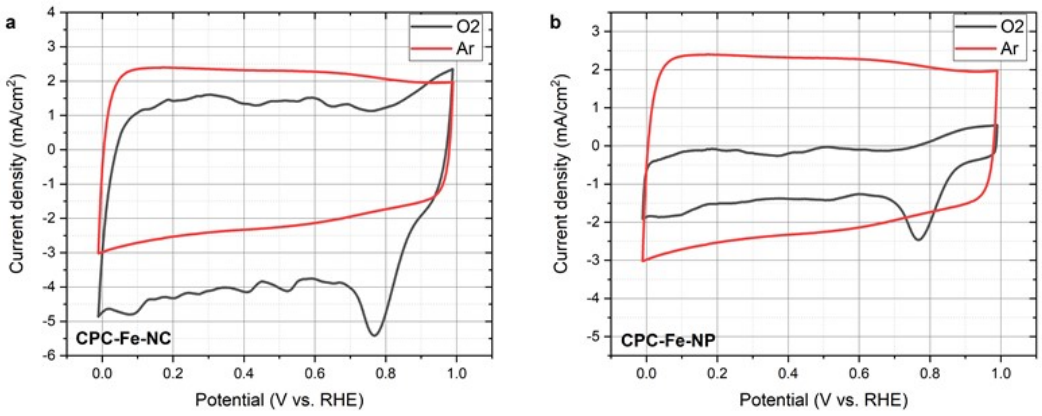

Figure S3. (a,b) CV curves of CPC-Fe-NC and CPC-Fe-NP under Ar and oxygen in 0.1 M KOH at 50 mV/s.

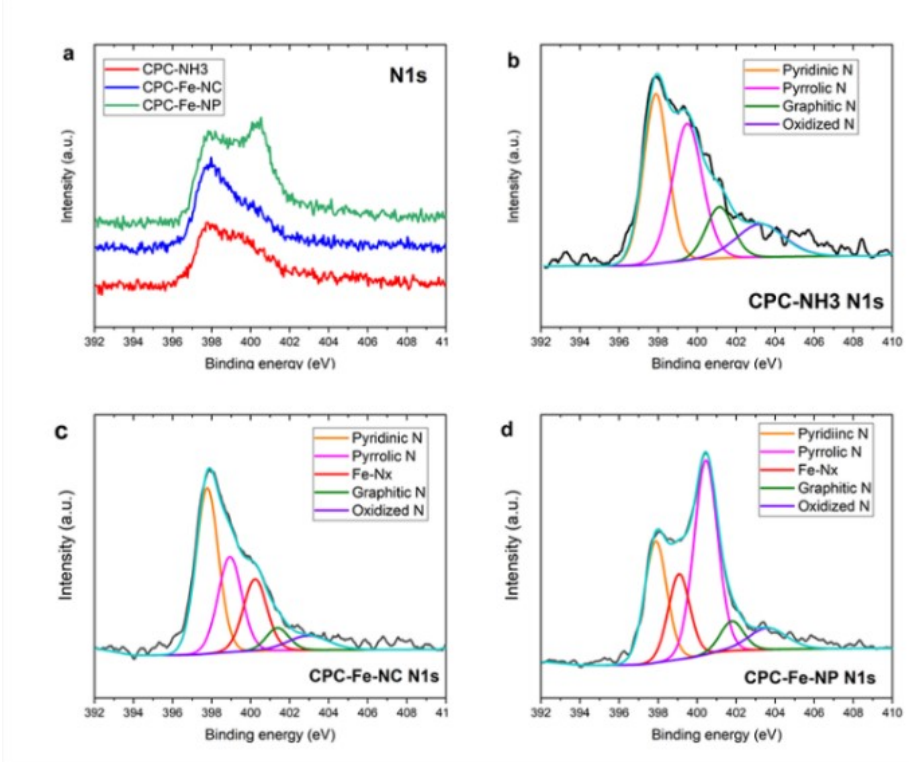

Figure S4. (a) XPS N1s spectra for CPC-NH3, CPC-Fe-NC, and CPC-Fe-NP, (b-d) Deconvoluted N1s spectra for CPC, CPC-NH3, CPC-Fe-NC, and CPC-Fe-NP.

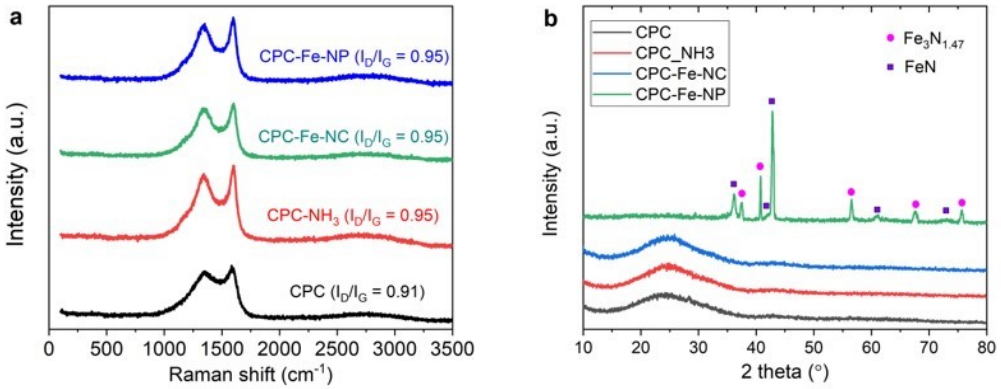

Figure S5. Raman and XRD spectra of CPC, CPC-NH3, and CPC-Fe-NC.

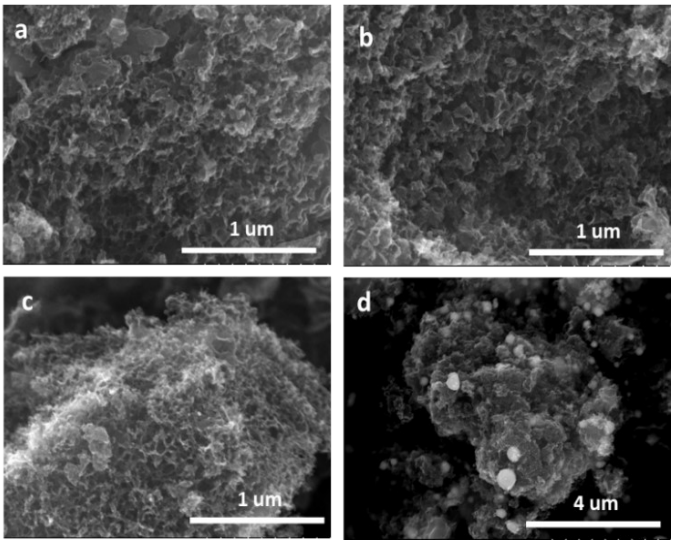

Figure S6. SEM images of (a) CPC, (b) CPC-NH3, (c) CPC-Fe-NC, and (d) CPC-Fe-NP.

Table S1. BET analysis results ([a] Total pore volume up to $P/P^0 \sim 0.995$, [b] t-plot micropore volume, [c] BJH desorption cumulative volume of pores).

	BET surface area	Total pore volume[a]	Micropore volume[b]	Mesopore volume[c]
unit	m^2/g	cm^3/g	cm^3/g	cm^3/g
CPC	894	2.74	0.124	2.405
CPC-NH3	914	2.97	0.121	2.637
CPC-Fe-NC	924	2.56	0.131	2.257
CPC-Fe-NP	375	1.02	0.064	0.849

Table S2. BET surface area, total pore volume, micropore area of CPC(1:1), CPC(1.5:1), and CPC(2:1).

	BET surface area (m^2/g)	Total pore volume (cm^3/g)[a]	T-plot micropore volume (cm^3/g)
CPC(1:1)	747	2.23	0.080
CPC(1.5:1)	764	2.72	0.068
CPC(2:1)	894	2.75	0.124

[a] Total pore volume up to $P/P_0 \sim 0.995$

Table S3. XPS N1s atomic percentage of deconvoluted peaks of CPC-NH3, CPC-Fe-NC and CPC-Fe-NP.

Sample	Peak BE (eV)	FWHM (eV)	Atomic %	Peak	
CPC-NH3	397.8	1.5	37.09	Pyridinic N	-
	399.4	1.8	36.53	Pyrrolic N	
	401.1	1.6	12.31	Graphitic N	
	403.2	2.9	14.07	Oxidized N	
CPC-Fe-NC	Peak BE (eV)	FWHM (eV)	Atomic %		Peak
	397.7	1.3	42.2	42.2	Pyridinic N
	398.9	1.4	45.1	25.8	$Fe\text{-}N_x$
	400.2	1.4		19.3	Pyrrolic N
	401.3	1.3	5.8	5.8	Graphitic N
	402.9	2.4	6.7	6.7	Oxidized N
CPC-Fe-NP	397.8	1.3	25.3	25.3	Pyridinic N
	399.0	1.3	60.4	17.3	$Fe\text{-}N_x$
	400.4	1.4		43.1	Pyrrolic N
	401.7	1.4	6.4	6.4	Graphitic N
	403.6	2.2	7.6	7.6	Oxidized N

Table S4. XPS overall atomic percentage of CPC, CPC-NH3, CPC-Fe-NC and CPC-Fe-NP.

(at.%)	CPC	CPC-NH3	CPC-Fe-NC	CPC-Fe-NP
C1s	89.7	89.08	90.73	87.92
O1s	7.39	6.12	4.97	6.35
N1s	0	4.01	3.08	3.03
Cl2p	0.53	0.46	0.47	0.34
B1s	2.38	0.32	0.75	1.34
Fe2p	-	-	-	1.02
N/C		0.045	0.034	0.034
Sum	100	100	100	100

Table S5. The overall atomic percentage of CPC measured by elemental analysis (EA).

(wt.%)	CPC
C1s	89.274
O1s	4.921
N1s	0.079

Table S6. Mass activity and onset potentials for the ORR with the catalysts under study and some of the best catalysts reported (a 20 wt.% Pt/C, b measured at 1500 ~ 1600 rpm).

Catalyst	$E_{1/2}$ (V)	$E_{1/2}$ of Pt/C (V)[a]	i_L @ 0.4V (mA/cm^2)[b]
CPC-Fe-NC (this work)	0.87	0.88	5.3
EDTA-based Fe-N-C[1]	0.80	0.75, 10 wt.%	4.8
α-Mn_2O_3/FeNC[2]	0.83	-	5.3
Mesoporous Fe-N/C[3]	0.84	0.84	5.6
Fe + Bipyr/C[4]	0.87	0.88	-
Fe-N_x/CNT/rGO[5]	0.86	0.84	4.3
Single atom Fe/N-C[6]	0.85	0.88	5.8

References

1 R. Gokhale, Y. Chen, A. Serov, K. Artyushkova and P. Atanassov, *Electrochem. commun.*, 2016, **72**, 140–143.

2 P. G. Santori, F. D. Speck, S. Cherevko, H. A. Firouzjaie, X. Peng, W. E. Mustain and F. Jaouen, *J. Electrochem. Soc.*, 2020, **167**, 134505.

3 C. Guo, Y. Li, Z. Li, Y. Liu, Y. Si and Z. Luo, *Nanoscale Res. Lett.*, 2020, **15**, 21.

4 R. Jäger, P. E. Kasatkin, E. Härk, P. Teppor, T. Romann, R. Härmas, I. Tallo, U. Mäeorg, U. Joost, P. Paiste, K. Kirsimäe and E. Lust, *J. Electroanal. Chem.*, 2018, **823**, 593–600.

5 X. Deng, M. Xiao, R. Yang, F. Guo, H. Chen, Y. Hu, Y. Li, C. Zhu, Y. Deng, Z. Jiang, Z. Xu, C. Gao, Q. He, J. Ge, Y. Hou, X. Zhang and Z. Chen, *J. Electrochem. Soc.*, 2018, **165**, F401–F407.

6 L. Yang, D. Cheng, H. Xu, X. Zeng, X. Wan, J. Shui, Z. Xiang and D. Cao, *Proc. Natl. Acad. Sci.*, 2018, **115**, 6626 LP – 6631.